ELSEVIER

Journal of Power Sources 62 (1996) 21–26

JOURNAL OF POWER SOURCES

Electrochemical properties and performance of poly(acrylonitrile)-based polymer electrolyte for $Li/LiCoO_2$ cells

Hyung Sun Kim [a], Byung Won Cho [a], Jung Taek Kim [a], Kyung Suk Yun [a], Hai Soo Chun [b]

[a] *Division of Chemical Engineering, Korea Institute of Science and Technology, PO Box 131, Cheongryang Seoul, South Korea*

[b] *Department of Chemical Engineering, Korea University, 1, Anam-dong Seoul, South Korea*

Received 8 December 1995; accepted 29 January 1996

Abstract

It has been demonstrated that $LiCoO_2$ is a very attractive cathode active material for lithium rechargeable cells. Poly(acrylonitrile) (PAN)-based polymer electrolyte is used for $Li/LiCoO_2$ cells. PAN-based polymer electrolyte shows ionic conductivity of the order 1 mS cm^{-1} at room temperature, irrespective of time evolution, and wide electrochemical stability up to 4.3 V (versus Li^+/Li). An $LiCoO_2$ composite cathode containing 4 wt.% conductive material displays a good cycling performance. From a.c. impedance results, the interfacial resistance of $Li/LiCoO_2$ cells is dominated by the passive layer formed at the lithium/polymer electrolyte interface.

Keywords: Polymer electrolytes; Composite cathodes; Lithium batteries; Lithium cobalt dioxide

1. Introduction

A flat-type lithium rechargeable battery using a polymer electrolyte and $LiCoO_2$ to intercalate lithium ions is a promising candidate battery for electric vehicles and portable electronic equipment. The primary advantages of this cell are a high voltage (4 V), a theoretical energy density of 1103 Wh l^{-1}, and a specific energy of 1070 Wh kg^{-1} [1,2]. Other advantages over conventional liquid-based batteries include: safety, light weight, flexible design, and relatively low cost.

One of the problems with these cells is a progressive capacity decline upon cycling. Although various authors have investigated this unfavourable effect with different cathode material systems [3,4], there is not clear explanation since, theoretically, the intercalating compounds support a very reversible process. Hooper et al. [5] have reported that the decline in capacity with cycling of Li/V_6O_{13} cells is associated with morphological changes in the composite cathode, rather than reduction of the extent of the intercalation process.

Therefore, in order to obtain stable capacity on cycling, it is necessary to improve the stability of the composite cathode materials at the operating voltage. It has been previously reported that the role of conductive material in the composite cathode material should be emphasized in order to achieve a high reversible capacity. This effect may be related to the limited number of available electron sites due to the low electronic conductivity of the active material [6,7].

In recent years, considerable effort has been devoted to the synthesis and characterization of polymer electrolytes and their application in the development of advanced lithium polymer batteries. To be practical, the polymer electrolyte must have a conductivity of 1×10^{-3} S cm^{-1} at room temperature. This performance is very unlikely with conventional polymer electrolytes such as poly(ethylene oxide) and related compounds. Among the most promising of the new types of polymer electrolyte is the gel-type, e.g. a poly(vinylidene fluoride) and poly(acrylonitrile) matrix that contains lithium salts in organic solvents such as ethylene carbonate (EC), propylene carbonate (PC), γ-butyrolactone. These gel electrolytes were originally described by Feuillade and Perche [8] and were further characterized by Watanabe et al. [9]. The latter reported that the ionic conductivity of the hybrid film does not correlate with the content of $LiClO_4$ in the PAN, but with the mole ratio EC:$LiClO_4$ in the films. When the ratio is about 2, the conductivity attains 10^{-4}–10^{-5} S cm^{-1} at room temperature. Abraham and Alamgir [10] reported that the ionic conductivity can be as high as 1×10^{-3} S cm^{-1} at room temperature when the ratio is increased. In addition to high ionic conductivity, the polymer electrolyte must have a wide electrochemical stability window since the electrode potential of $LiCoO_2$ becomes higher than 4 V (versus Li^+/Li).

This work characterizes the electrochemical properties of the polymer electrolyte and examines the effect of conductive

PII S0378-7753(96)02393-2

material in the composite cathode on the cycling performance of a lithium polymer battery.

2. Experimental

The composite cathodes consisted of $LiCoO_2$ as an active material (Cyprus Foote Mineral, CFM), Ketjen black (Mitsubishi Chemical Co.) as a conductor, and polymer electrolyte as a binder. Cathode films were prepared by casting the appropriate ethyl alcohol slurry on an aluminum foil (thickness 18 μm) current-collector.

One composite cathode had a composition of 40 wt.% $LiCoO_2$ active material, 4 wt.% Ketjen black and 56 wt.% polymer electrolyte. The other cathode had a composition of 42 wt.% $LiCoO_2$, 2 wt.% Ketjen black and 56 wt.% polymer electrolyte. Both electrodes had a surface area of 2 cm^2 (diameter 1.6 cm) and contained 3 mg cm^{-2} of $LiCoO_2$ active material.

The polymer electrolyte consisted of a PAN matrix, an $LiPF_6$ lithium salt, and an EC and PC mixture. The PAN powder and lithium salt were first dissolved in the solvent mixture of EC and PC at elevated temperature. The electrolyte film was prepared by casting the viscous polymer solution with a doctor blade on a stainless-steel plate.

Lithium polymer cells using a lithium foil anode (CFM) with a thickness of 125 μm were constructed and sealed in a dry argon box. A schematic of the prototype lithium polymer cell is shown in Fig. 1; its actual form is shown in Fig. 2.

Impedance measurements were performed over the frequency range 65 kHz to 0.1 Hz by a Solartron 1260 frequency response analyser in combination with a 1286 electrochemical interface and an IBM computer.

The electrochemical stability window of the polymer electrolyte was investigated by cyclic voltammetry using a 173 PAR potentiostat/galvanostat and a 175 universal programmer. This measurement was carried out on a stainless-steel working electrode with lithium electrodes as the counter and reference electrodes.

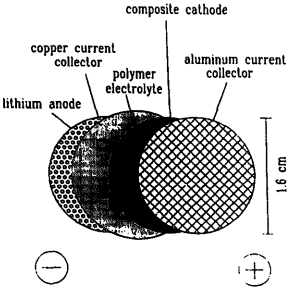

Fig. 1. Schematic diagram of the structure of a prototype lithium polymer cell.

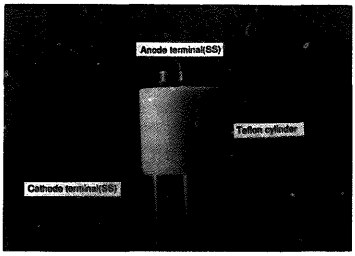

Fig. 2. Sealed lithium polymer cell.

The cycle test was conducted in the voltage range 3.0–4.3 V by galvanostatically controlled equipment.

3. Results and discussion

The impedance spectra of an Li/PE/Li cell at various times under open-circuit potential (OCP) conditions at room temperature are given in Fig. 3. It is well known that the resistance of the cell is composed of the bulk resistance, R_b, of the polymer electrolyte and the interfacial resistance, R_i, which reflects the interfacial situation between the electrode and the electrolyte [11]. At high frequency, the line intercepts the real part (Z') and this point corresponds to the bulk resistance of the polymer electrolyte. This allows calculation of the ionic conductivity of the polymer electrolyte with a cell constant value of 0.005 cm^{-1}. The electrolyte maintained a conductivity of the order 1×10^{-3} S cm^{-1} at room temperature, irrespective of time. This means that the encapsulated liquid electrolyte in the polymer chains has not lost its electrochemical properties because of the non-volatile nature of the

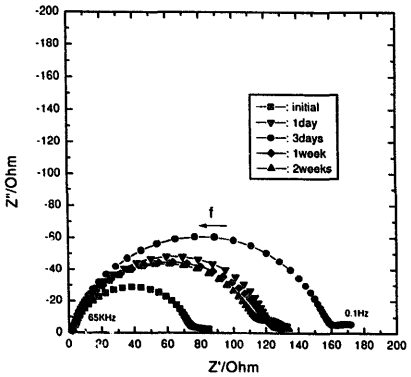

Fig. 3. A.c. impedance spectrum of an Li/PE/Li cell with time at room temperature.

organic solvent and exhibits good compatibility with the lithium electrode.

The value of R_i increased quickly for the first three days and stabilized at a value of 240 $\Omega\,cm^2$ after two weeks. This phenomenon can be attributed to the formation of a passive layer due to the reactivity of the electrode and the electrolyte.

The interfacial capacitance, C_i, is easily calculated from Eq. (1). The value is independent of time and reaches value of about 1 $\mu F\,cm^{-2}$

$$C_i = \frac{1}{R_i \omega_{max}} \quad (1)$$

where ω_{max} is the maximum angular frequency of the semicircle; the magnitudes of the resistor and capacitor are equal.

The apparent thickness of the passive layer can be calculated according to the following equation [12]:

$$L = \frac{\epsilon A}{C_i \pi 3.6 \times 10^{12}} \quad (2)$$

where L is the thickness of the passive layer, A the electrode area, and ϵ the dielectric constant of the passive layer. From Eq. (2), if the value of the dielectric constant is assumed to be 5, the thickness of the passive layer on the lithium electrode is about 45 Å. It has been reported that the thickness of the passive layer on freshly immersed lithium, magnesium and calcium electrodes in non-aqueous electrolytes is typically in the range of 25 to 100 Å[13].

The cyclic voltammogram for the Li/PE/SS cell at room temperature is given in Fig. 4. The sweep rate is 5 mV s^{-1}. The first cathodic peak current is observed at around 1.5 V, which corresponds to the decomposition of moisture in the electrolyte. Prior to plating lithium on the stainless-steel electrode at −0.18 V, the reduction charge is about 30 mC cm^{-2}. According to Meitav and Peled[14], plating of lithium on such an electrode takes place only after prior formation of a solid electrolyte interphase on the electrode by the passage of at least 20 mC cm^{-2} in 1 M $LiAlCl_4$–$SOCl_2$ solution. This value is in good agreement with those calculated in the system studied here.

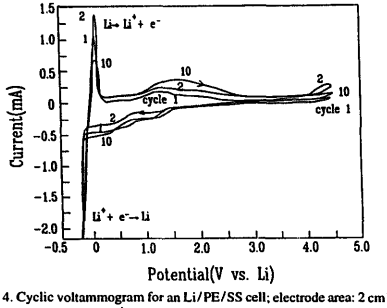

Fig. 4. Cyclic voltammogram for an Li/PE/SS cell; electrode area: 2 cm^{-2}, and sweep rate: 5 mV s^{-1}.

On the reverse scan, stripping of lithium is observed at around 0.28 V. This plating-stripping process is reversible, the kinetics are fast but the reversibility tends to decrease with cycling. As can be seen in Fig. 4, there are no more oxidation peaks up to 4.3 V (versus Li^+/Li). The electrolyte oxidation current increases after the first cycle and stabilizes at lower values after ten cycles. This phenomenon may result from the formation of a passivating layer on the stainless-steel electrode. Thus, the PAN-based polymer electrolyte in this work has displayed sufficient electrochemical stability to allow safe operation in rechargeable lithium battery systems.

Generally, the oxidative stability of organic esters (such as EC and PC) is higher than that of ethers. Croce et al. [15] reported that the addition of PAN appears to influence the oxidation potential and the PAN–$LiClO_4$-based electrolyte has higher electrochemical stability than any of the other PAN–lithium salt based electrolytes. This has also been observed in our laboratories [16].

It is considered that the number of free lithium ions encapsulated in the polymer chain influences the interaction between the polymer and the lithium salts. Recent IR measurements also imply some interaction between lithium ions and the polar portion of the PAN chain which corresponds to C≡N stretch modes [17]. Since the $LiClO_4$ lithium salt has a higher lattice energy than any of the other lithium salts, the interaction between the polymer and the lithium salt is relatively small; this effect influences the electrochemical stability window. On the other hand, its explosive property in the presence of organic solvent, especially when the solvents are in a low concentration, introduces a serious hazard during the construction and use of cells based on this electrolyte. Although $LiPF_6$ has the lowest thermal stability of all lithium salts and greater sensitivity to moisture, the electrochemical oxidative stability is adequate and there is less corrosion with an aluminum current-collector. Tarascon and Guyomard [18] have recently reported that $LiPF_6$ in a mixture of EC and PC is electrochemically stable in the presence $LiMn_2O_4$ to well beyond 5.1 V (versus Li^+/Li).

The cycling performance of two different composite cathode formulations with 4 or 2 wt.% of Ketjen black, is shown in Fig. 5.

The overall reaction of $LiCoO_2$ is given by Eq. (3) and the calculated capacity is 125 mAh g^{-1}

$$Li_{0.55}CoO_2 + 0.45Li^+ + 0.45e^- \Leftrightarrow LiCoO_2$$
$$125 mAh\,g^{-1} \quad (3)$$

The corresponding specific capacities are close to the calculated capacity value, as shown in Fig. 5. When more than 0.45 of lithium is extracted from these compounds, Co^{3+} is easily oxidized to Co^{4+} and this destroys the crystallinity of the cathode and, hence, decreases the reversibility of the cell [19]. Therefore, the depth-of-discharge is limited to less than 125 mAh per g of $LiCoO_2$ to sustain the cycling performance.

Cell A and cell B, which contain 4 and 2 wt.% of conductive material, respectively, display different performance, as

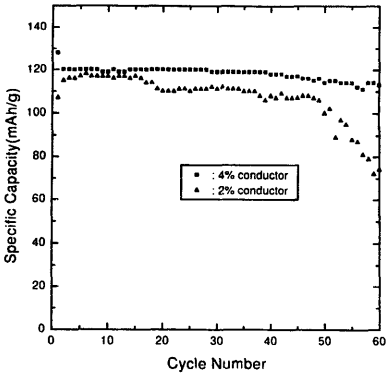

Fig. 5. Cycling performance of Li/PE/$LiCoO_2$ cells with conductive material contents at $C/8$ rate.

shown in Fig. 5. During the initial ten cycles, the specific capacities are similar to each other, but the capacity of cell B then tends to decrease rapidly with further cycling. Excellent material utilization is achieved in cell A. Saidi and Barker [6] have reported that composite cathodes based on V_6O_{13} with a suitable amount of conductive carbon (10 wt.% Shiwinigan black) deliver excellent discharge capacities at low discharge rates, whereas the utilization of a composite V_6O_{13} cathode with no conductive carbon displays a significantly lower discharge capacity due to electrode polarization effects. This is consistent with the poor intrinsic electronic conductivity of the composite $LiCoO_2$ cathode.

The voltage profiles of cell A and cell B at the 20th cycle are given in Fig. 6. Clearly, the voltage of cell B is higher than that of cell A. This effect is associated with the progressive decline in capacity due to the electrical isolation of some active material within the composite cathode. The cycling performance of cell A at a different cycling rates is presented in Fig. 7. Upon cycling, the discharge capacity is constant at the $C/8$ and $C/4$ rates. At the $C/2$ rate, however, the capacity is slightly less than that at a low rate; it declines rapidly after 50 cycles. It is concluded that the reduced capacity at high rates is due to the low value of the chemical diffusion coefficient of lithium ions in the lattice of $LiCoO_2$. This value has been measured by various authors who have employed different measuring techniques. Mizushima et al. [20] reported a value of $5 \times 10^{-9}\,cm^2\,s^{-1}$ using a transient technique, while Thomas et al. [21] obtained a value of $5 \times 10^{-8}\,cm^2\,s^{-1}$ by impedance spectroscopy.

Typical voltage profiles for cell A at different cycling rates are given in Fig. 8. These profiles are similar to the profiles of lithium/liquid electrolyte/$LiCoO_2$ cells. This means that the magnitude of polarization and capacity during both charge and discharge of the polymer electrolyte system are the same as those of other liquid electrolyte systems. Also, the pattern of the voltage profiles does not change after prolonged cycling. The mean operating voltage is about 3.90 V at both the $C/8$ and $C/4$ rates, and about 3.85 V at the $C/2$ rate.

The impedance spectrum of cell A before and after one cycle is shown in Fig. 9. The spectrum consists of two semicircles. The larger semicircle, in the middle-frequency region, is attributed to the interfacial resistance at the lithium anode. The impedance spectrum of an Li/PE/Li cell exhibits a similar pattern, as shown in Fig. 10. On the other hand, the smaller semicircle in the high-frequency range corresponds to the impedance of a surface layer formed on the cathode surface. Goodenough et al. [22] have reported that this surface layer consists of a 30 Å thick amorphous layer that surrounds the $LiCoO_2$ particles in 1 M $LiBF_4$/PC solution and is independent of the applied voltage. Therefore, it can

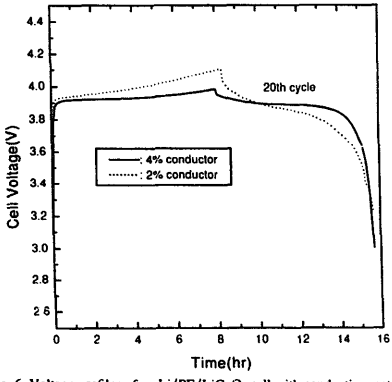

Fig. 6. Voltage profiles of an Li/PE/$LiCoO_2$ cell with conductive material contents at $C/8$ rate.

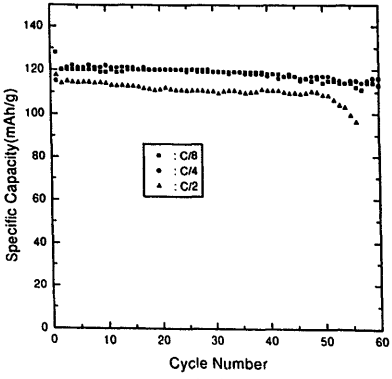

Fig. 7. Cycling performance of an Li/PE/$LiCoO_2$ cell A at different cycling rates.

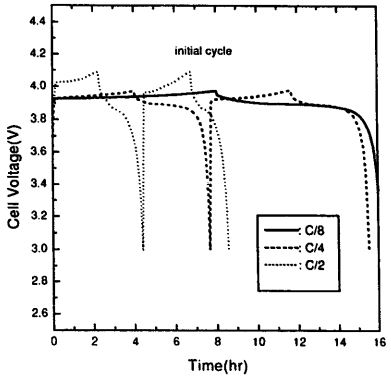

Fig. 8. Voltage profiles of an Li/PE/$LiCoO_2$ cell A at different cycling rates.

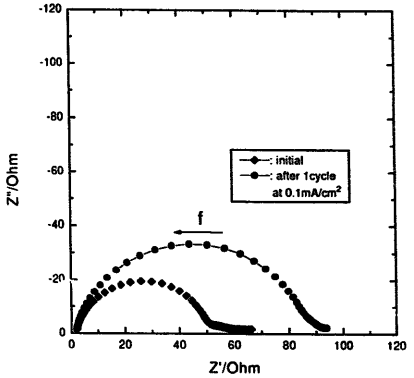

Fig. 10. A.c. impedance spectrum of an Li/PE/Li cell.

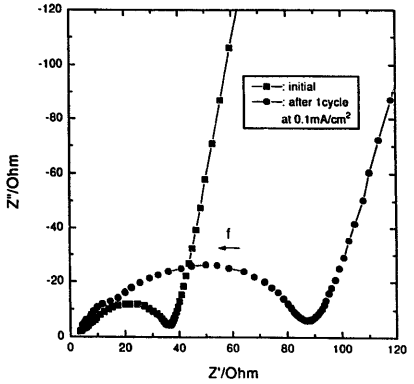

Fig. 9. A.c. impedance spectrum of the Li/PE/$LiCoO_2$ cell A.

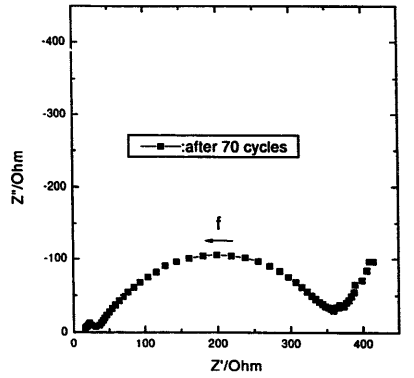

Fig. 11. A.c. impedance spectrum of the Li/PE/$LiCoO_2$ cell A after prolonged cycling.

be associated with bulk ionic conduction. At low frequency, the behaviour is associated with that of a rough blocking $LiCoO_2$ electrode. Hardy and Shriver [23] observed similar low-frequency behaviour in poly(diallyldimethylammonium). Nagasubramanian and De Stefano [24] accounted for this non-ideal spur by invoking the constant phase element impedance.

The impedance spectrum of cell A after 70 cycles is shown in Fig. 11. The semicircle assigned to the lithium anode interface becomes larger with further cycling. Therefore, it is concluded that the interfacial resistance of the cell is dominated by a passive layer formed at the lithium/polymer electrolyte interface. The progressive decline in capacity can be explained by electrical isolation of the available $LiCoO_2$ particles.

4. Conclusions

PAN-based polymer electrolyte displays electrochemical properties that are sufficient to allow operation in an Li/$LiCoO_2$ cell.

An $LiCoO_2$ composite cathode containing 4 wt.% conductive material (Ketjen black) has high material utilization and good cycling performance. A cell containing 2 wt.% conductive material is found to have relatively low cycle life and capacity due to electrical isolation of the available active material.

The interfacial resistance of the Li/$LiCoO_2$ cell with cycling is dominated mainly by the passive layer formed at the lithium/polymer electrolyte interface.

Acknowledgements

The authors are grateful for the financial support of the Ministry of Science and Technology, South Korea.

References

[1] K. Brandt, *Solid State Ionics, 69* (1994) 173.
[2] E. Plichta, M. Salomon, S. Slane, M. Uchiyama, D. Chan and W.H. Lian, *J. Power Sources, 21* (1987) 25.
[3] M.Z.A. Munshi and B.B. Owens, *Solid State Ionics, 20* (1988) 41.
[4] K. West, B. Zachau-Christiansen and T. Jacobsen, *J. Power Sources, 14* (1987) 165.
[5] A. Hooper and B.C. Tofield, *J. Power Sources, 11* (1984) 33.
[6] M.Y. Saidi and J. Barker, *Solid State Ionics, 78* (1995) 169.
[7] K. West, B. Zachau-Christiansen and T. Jacobsen, *Electrochim. Acta, 28* (1983) 1829.
[8] G. Feuillade and Ph. Perche, *J. Appl. Electrochem., 5* (1975) 63.
[9] M. Watanabe, M. Kanbe, K. Nagaoka and I. Shinora, *J. Polym. Sci. Polym. Physics, 21* (1983) 939.
[10] K. M. Abraham and M. Alamgir, *J. Electrochem. Soc., 137* (1990) 1657.
[11] G. Nagasubramanian, A.I. Attia and G. Halpert, *J. Appl. Electrochem., 24* (1994) 298.
[12] E. Peled and H. Straze, *J. Electrochem. Soc., 124* (1077) 1030.
[13] E. Peled, in J.P. Gabano (eds.), *Lithium Batteries*, Academic Press, London, 1983, p. 43.
[14] A. Meitav and E. Peled, *J. Electroanal. Chem., 134* (1982) 49.
[15] F. Croce, F. Gerace, G. Dautzenberg, S. Passerini, G.B. Appetecchi and B. Scrosati, *Electrochim. Acta, 39* (1994) 2187.
[16] H.S. Kim, B.W. Cho, K.S. Yun and H.S. Chun, *Theories and Application of Chemical Engineering*., KIChE, 1 (1995) 49.
[17] F. Croce, S.D. Brown, S.G. Greenbaun, S.M. Slane and M. Salomon, *Chem. Mater., 5* (1993) 1268.
[18] J.M. Tarascon and D. Guyomard, *Solid State Ionics, 69* (1994) 293.
[19] J.N. Reimers and J.R. Dahn, *J. Electrochem. Soc., 139* (1992) 2091.
[20] K. Mizushima, P.J. Wiseman, P.C. Jones and J.B. Goodenough, *Solid State Ionics, 3/4* (1981) 171.
[21] M.G.S.R. Thomas, P.G. Bruce and J.B. Goodenough, *Solid State Ionics, 18/19* (1986) 794.
[22] M.G.S.R. Thomas, P.G. Bruce and J.B. Goodenough, *J. Electrochem. Soc., 132* (1985) 1521.
[23] L.C. Hardy and D. F. Shriver, *J. Am. Chem. Soc., 107* (1985) 3823.
[24] G.Nagasubramanian and S. Di Stefano, *J. Electrochem. Soc., 137* (1990) 3830.